DEPARTMENT OF MECHANICAL ENGINEERING AND MECHANICS
SCHOOL OF ENGINEERING
OLD DOMINION UNIVERSITY
NORFOLK, VIRGINIA 23508

NUMERICAL SOLUTIONS OF NAVIER-STOKES EQUATIONS FOR A BUTLER WING

By

Jamshid S. Abolhassani, Graduate Research Assistant

and

S. N. Tiwari, Principal Investigator

Progress Report
For the period ending August 31, 1985

Prepared for the
National Aeronautics and Space Administration
Langley Research Center
Hampton, Virginia 23665

Under
Research Grant NCC1-68
Dr. Robert E. Smith, Jr., Technical Monitor
ACD-Computer Applications Branch

Submitted by the
Old Dominion University Research Foundation
P.O. Box 6369
Norfolk, Virginia 23508

October 1985

FOREWORD

This is a progress report on the research project "Numerical Solutions of Navier-Stokes Equations for a Butler Wing." The period of performance on this research was January 1 through August 31, 1985. The work is supported by the NASA/Langley Research Center through Cooperative Agreement NCC1-68, and monitored by Dr. Robert E. Smith, Jr., of the Analysis and Computation Division (Computer Applications Branch), NASA/Langley, MS/125.

ABSTRACT

The flow field is simulated on the surface of a given delta wing (Butler wing) at zero incident in a uniform stream. The simulation is done by integrating a set of flow field equations. This set of equations governs the unsteady, viscous, compressible, heat conducting flow of an ideal gas. The equations are written in curvilinear coordinates so that the wing surface is represented accurately. These equations are solved by the finite difference method, and results obtained for high-speed freestream conditions are compared with theoretical and experimental results.

In the present study, the Navier-Stokes equations are solved numerically. These equations are unsteady, compressible, viscous, and three-dimensional without neglecting any terms. The time dependency of the governing equations allows the solution to progress naturally for an arbitrary initial guess to an asymptotic steady state, if one exists. The equations are transformed from physical coordinates to the computational coordinates, allowing the solution of the governing equations in a rectangular parallelepiped domain. The equations are solved by the MacCormack time-split technique which is vectorized and programmed to run on the CDC VPS 32 computer. The codes are written in 32-bit (half word) FORTRAN, which provides an approximate factor of two decrease in computational time and doubles the memory size compared to the 64-bit word size.

TABLE OF CONTENTS

LIST OF FIGURES

TABLE OF CONTENTS - continued -

LIST OF FIGURES - continued

NUMERICAL SOLUTIONS OF NAVIER-STOKES EQUATIONS FOR A BUTLER WING

By

J. S. Abolhassani[1] and S. N. Tiwari[2]

1. INTRODUCTION

The Butler wing is a delta wing which was proposed by D. S. Butler (Ref. 4). The planform of the body is an isosceles triangle, and the leading edges of the wing are laid along the Mach lines of the undisturbed stream. For the first 20% of the length, the body is a right circular cone. The remainder of the body has elliptic sections which become more eccentric as the sharp trailing edges are approached.

D. S. Butler has compared experimental results for surface pressure with theoretical values obtained by using a characteristic method to integrate an approximate form of the inviscid equations of motion (Ref. 4). Butler used the hypersonic slender body theory approximation to simplify the full equations of motions. Walkden and Caine estimated the pressure on the surface of a Butler wing at zero incident in a steady uniform stream by numerically integrating the two semi-characteristic forms of equations which govern the inviscid supersonic flow of an ideal gas with constant specific heat (Ref. 5). Squire obtained experimental results for a Butler wing at different Mach numbers and different angles of attach (Ref. 6,7). All previous numerical investigations have used inviscid equations and have excluded the wake region. In contrast, this study investigates the wake region as well as the effect of viscosity on the flow. The results of this study are compared with available experimental and numerical results.

---

[1]Graduate Research Assistant, Department of Mechanical Engineering and Mechanics, Old Dominion University, Norfolk, Virginia 23508.
[2]Eminent Professor, Department of Mechanical Engineering and Mechanics, Old Dominion University, Norfolk, Virginia 23508.

In order to study the flow around a Butler wing, the Navier-Stokes equations are solved numerically. These equations are unsteady, compressible, viscous, and three-dimensional without neglecting any terms. The time dependency of the governing equations allows the solution to progress naturally from an arbitrary initial guess to an asymptotic steady state, if one exists. The equations are transformed from the physical coordinates to the computational coordinates, allowing the solution of the governing equations in a rectangular parallelepiped domain. The equations are solved by the McCormack time-split technique which is vectorized and programmed to run on the CDC VPS 32 (CYBER 205) computer. The codes were written in the 32-bit (half-word) FORTRAN which provides an approximate factor of two, decrease in computer time, and doubles the memory compared to the 64-bit word size.

2. GOVERNING EQUATIONS

The governing equations for a thermal fluid system are the conservation of mass, momentum, and energy. These equations are developed for an arbitrary region assuming the system is in continuum. Equations of motion for viscous, compressible, unsteady, heat conducting flow can be written as:

Continuity: $$\frac{\partial \rho}{\partial t} + \nabla \cdot (\rho \bar{u}) = 0, \tag{2.1}$$

Momentum: $$\frac{\partial (\rho \bar{u})}{\partial t} + \nabla \cdot (\rho \bar{u}\bar{u} - \tau) = 0, \tag{2.2}$$

Energy: $$\frac{\partial (E)}{\partial t} + \nabla \cdot (E\bar{u} + \bar{q} - \bar{u} \cdot \tau) = 0, \tag{2.3}$$

where E is the total energy per unit volume given by $E = \rho \left(e + \frac{V^2}{2} + \text{potential energy} + \ldots\right)$ and e is the internal energy per unit volume. Equations 2.3 can be simplified by assuming that the stress at a point is linearly dependent on the rate of strain (deformation) of the fluid (Newtonian fluid),

$$\tau_{ij} = - P \delta_{ij} + \mu \left(\frac{\partial u_i}{\partial x_j} + \frac{\partial u_j}{\partial x_i} \right) + \delta_{ij} \mu' \frac{\partial u_k}{\partial x_k} \Big] . \tag{2.4a}$$

where δ_{ij} is the Kronecker delta function, and μ' is the second coefficient of viscosity. The two coefficients are related to the coefficient of bulk viscosity (k) by the expression $k = 2\mu/3+\mu'$. The contribution of k can be neglected if the pressure in a fluid is not changed abruptly during

its expansion or contractions. Under this assumption, the stress tensor can be related to the pressure and velocity components as:

$$\tau_{ij} = - P \delta_{ij} + \mu \left[\left(\frac{\partial u_i}{\partial x_j} + \frac{\partial u_j}{\partial x_i} \right) - \frac{2}{3} \delta_{ij} \frac{\partial u_k}{\partial x_k} \right] . \qquad (2.4b)$$

This equation is valid for continuum flows. For an isotropic system, the heat flux in Eq. (2.3) can be expressed in terms of temperature gradient (Fourier's law of heat conduction) as:

$$q = - K \nabla T \qquad (2.5)$$

where K is the coefficient of thermal conductivity. A common approximation used for viscosity is based on the kinetic theory of gases using an idealized intermolecular-forces potential. The relation is:

$$\frac{\mu}{\mu_r} = \left(\frac{T}{T_r}\right)^{3/2} \frac{T_r + S_o}{T + S_o} \qquad (2.6)$$

where

$$S_o = 198.6^\circ R$$

$$\mu_r = 0.1716 \text{ mp}$$

coefficients of thermal conductivity K can be determined from Prandtl number

$$K = \frac{\gamma \mu C_v}{Pr} \qquad (2.7)$$

where C_v is the specific heat at constant volume and γ is the ratio of specific heats.

It is necessary to have a supplementary relation to close the system of equations (Eq. (2.1) - (2.3)). By neglecting intermolecular forces (a thermally perfect system), thermodynamic properties can be related as:

$$P = \rho RT \tag{2.8}$$

where R is the gas constant. Thermally perfect gas assumption allows expression of the internal energy (e) as a function of T only [$e = e(T)$]. In addition, assumption of calorically perfect gas [$e(0) = 0$] allows the following relation:

$$e = C_v T. \tag{2.9}$$

A combination of Eqs. (2.8) and (2.9) results in

$$P = \rho e\,(\gamma-1). \tag{2.10}$$

These equations (Eqs. (2.1) - (2.3)) are in conservative form. For simplicity, these equations can be expressed into a compact vector form as:

$$\frac{\partial U}{\partial t} + \frac{\partial F}{\partial x} + \frac{\partial G}{\partial y} + \frac{\partial H}{\partial z} = 0, \tag{2.11}$$

where

$$U = \begin{bmatrix} \rho \\ \rho u \\ \rho v \\ \rho w \\ E \end{bmatrix}, \qquad F = \begin{bmatrix} \rho u \\ \rho uu - \tau_{xx} + P \\ \rho uv - \tau_{xy} \\ \rho uw - \tau_{xz} \\ Eu + \dot{q}_x - \phi_x + Pu \end{bmatrix},$$

$$G = \begin{bmatrix} \rho v \\ \rho uv - \tau_{yx} \\ \rho vv - \tau_{yy} + P \\ \rho vw - \tau_{yz} \\ Ev + \dot{q}_y - \phi_y + Pv \end{bmatrix}, \qquad H = \begin{bmatrix} \rho w \\ \rho uw - \tau_{zx} \\ \rho vw - \tau_{zy} \\ \rho ww - \tau_{zz} + P \\ Ew + \dot{q}_z - \phi_z + Pw \end{bmatrix}.$$

For the sake of generality, we can transform these equations from a physical domain to a computational domain as

$$\frac{\partial U}{\partial t} + \begin{bmatrix} \xi_x \\ \xi_y \\ \xi_z \end{bmatrix} \left(\frac{\partial F}{\partial \xi}, \frac{\partial G}{\partial \xi}, \frac{\partial H}{\partial \xi} \right) + \begin{bmatrix} \eta_x \\ \eta_y \\ \eta_z \end{bmatrix} \left(\frac{\partial F}{\partial \eta}, \frac{\partial G}{\partial \eta}, \frac{\partial H}{\partial \eta} \right) \tag{2.12}$$

$$+ \begin{bmatrix} \zeta_x \\ \zeta_y \\ \zeta_z \end{bmatrix} \left(\frac{\partial F}{\partial \zeta}, \frac{\partial G}{\partial \zeta}, \frac{\partial H}{\partial \zeta} \right) = 0 .$$

The transformation coefficients can be computed from a functional relation between the computational coordinates and the physical coordinates.

$$x = x(\xi,\eta,\zeta), \quad y = y(\xi,\eta,\zeta), \quad \text{and} \quad z = z(\xi,\eta,\zeta). \tag{2.13}$$

$$\xi = \xi(x,y,z), \quad \eta = \eta(x,y,z), \quad \text{and} \quad \zeta = \zeta(x,y,z). \tag{2.14}$$

If Eq. (2.14) is known, the transformation coefficients can be computed by direct differentiation. If the former relation is not known, after some algebraic manipulation, the transformation coefficients can be computed by:

$$\begin{bmatrix} \frac{\partial \xi}{\partial x} & \frac{\partial \xi}{\partial y} & \frac{\partial \xi}{\partial z} \\ \frac{\partial \eta}{\partial x} & \frac{\partial \eta}{\partial y} & \frac{\partial \eta}{\partial z} \\ \frac{\partial \zeta}{\partial x} & \frac{\partial \zeta}{\partial y} & \frac{\partial \zeta}{\partial z} \end{bmatrix} = [J] = \begin{bmatrix} \frac{\partial x}{\partial \xi} & \frac{\partial x}{\partial \eta} & \frac{\partial x}{\partial \zeta} \\ \frac{\partial y}{\partial \xi} & \frac{\partial y}{\partial \eta} & \frac{\partial y}{\partial \zeta} \\ \frac{\partial z}{\partial \xi} & \frac{\partial z}{\partial \eta} & \frac{\partial z}{\partial \zeta} \end{bmatrix}^{-1} \tag{2.15}$$

where $[J]$ and $|J^{-1}|$ are defined as (see Appendix A)

$$[J] = \frac{1}{|J^{-1}|} \begin{bmatrix} \left(\frac{\partial y}{\partial \eta}\frac{\partial z}{\partial \zeta} - \frac{\partial y}{\partial \zeta}\frac{\partial z}{\partial \eta}\right) & -\left(\frac{\partial x}{\partial \eta}\frac{\partial z}{\partial \zeta} - \frac{\partial x}{\partial \zeta}\frac{\partial z}{\partial \eta}\right) & \left(\frac{\partial x}{\partial \eta}\frac{\partial y}{\partial \zeta} - \frac{\partial x}{\partial \zeta}\frac{\partial y}{\partial \eta}\right) \\ -\left(\frac{\partial y}{\partial \xi}\frac{\partial z}{\partial \zeta} - \frac{\partial y}{\partial \zeta}\frac{\partial z}{\partial \xi}\right) & \left(\frac{\partial x}{\partial \xi}\frac{\partial z}{\partial \zeta} - \frac{\partial x}{\partial \zeta}\frac{\partial z}{\partial \xi}\right) & -\left(\frac{\partial x}{\partial \xi}\frac{\partial y}{\partial \zeta} - \frac{\partial x}{\partial \zeta}\frac{\partial y}{\partial \xi}\right) \\ \left(\frac{\partial y}{\partial \xi}\frac{\partial z}{\partial \eta} - \frac{\partial y}{\partial \eta}\frac{\partial z}{\partial \xi}\right) & -\left(\frac{\partial x}{\partial \xi}\frac{\partial z}{\partial \eta} - \frac{\partial x}{\partial \eta}\frac{\partial z}{\partial \xi}\right) & \left(\frac{\partial x}{\partial \xi}\frac{\partial y}{\partial \eta} - \frac{\partial x}{\partial \eta}\frac{\partial y}{\partial \xi}\right) \end{bmatrix} \tag{2.16}$$

$$|J^{-1}| = \begin{bmatrix} \frac{\partial x}{\partial \xi} & \frac{\partial x}{\partial \eta} & \frac{\partial x}{\partial \zeta} \\ \frac{\partial y}{\partial \xi} & \frac{\partial y}{\partial \eta} & \frac{\partial y}{\partial \zeta} \\ \frac{\partial z}{\partial \xi} & \frac{\partial z}{\partial \eta} & \frac{\partial z}{\partial \zeta} \end{bmatrix}$$

$$= \frac{\partial x}{\partial \xi}\left(\frac{\partial y}{\partial \eta}\frac{\partial z}{\partial \zeta} - \frac{\partial y}{\partial \zeta}\frac{\partial z}{\partial \eta}\right) - \frac{\partial x}{\partial \eta}\left(\frac{\partial y}{\partial \xi}\frac{\partial z}{\partial \zeta} - \frac{\partial y}{\partial \zeta}\frac{\partial z}{\partial \xi}\right)$$

$$+ \frac{\partial x}{\partial \zeta}\left(\frac{\partial y}{\partial \xi}\frac{\partial z}{\partial \eta} - \frac{\partial y}{\partial \eta}\frac{\partial z}{\partial \xi}\right)$$

In the present case, the planes of grid are perpendicular to the x-direction thus allowing us to write:

$$x = x(\xi) \tag{2.17}$$

$$y = y(\eta,\zeta) \tag{2.18}$$

$$z = z(\eta,\zeta). \tag{2.19}$$

This reduces the metric coefficient from nine to five non-zero elements.

3. METHOD OF SOLUTION

A time marching method is used to compute the solution. This allows us to capture the possible transient feature. This method is an explicit second-order accurate time-split predictor-corrector algorithm [3]. The governing equations (Eq. (2.12)) are discretized in computational directions. In a compact form, they can be expressed as

$$U^{n+1}_{i,j,k} = \left[L_\eta(\Delta t_\eta)\right]\left[L_\zeta(\Delta t_\zeta)\right]\left[L_\xi(\Delta t_\xi)\right]\left[L_\zeta(\Delta t_\zeta)\right]\left[L_\eta(\Delta t_\eta)\right] U^{n}_{i,j,k} \qquad (3.1)$$

where

$$\Delta t_\eta = \Delta t_\zeta = \frac{1}{2}\Delta t_\xi$$

and L_ξ, L_η, and L_ζ are the operators in ξ, η, and ζ directions, respectively. A time step is completed in this algorithm with the application of each operator applied symmetrically about the middle operator. For example, operator L_ξ can be defined as

$$L_\xi(\Delta t_\xi) = U^{out}_{i,j,k} \qquad (3.2a)$$

where

Predictor step:

$$\bar{U}_{i,j,k} = U^{in}_{i,j,k} - \frac{\Delta t_\xi}{\Delta \xi}\left[(F_i - F_{i-1})\frac{\Delta \xi}{\partial x}\,i + (G_i - G_{i-1})\frac{\partial \xi}{\partial y}\,i + (H_i - H_{i-1})\frac{\partial \xi}{\partial z}\,i\right]_{j,k} \qquad (3.2b)$$

Corrector step:

$$U^{out}_{i,j,k} = \frac{1}{2}\left(U^{in}_{i,j,k} + \bar{U}_{i,j,k} - \frac{\Delta t_\xi}{\Delta\xi}\left[(F_{i+1} - F_i)\frac{\partial\xi}{\partial x}\,i + (G_{i+1} - G_i)\frac{\partial\xi}{\partial y}\,i + (H_{i+1} - H_i)\frac{\partial\xi}{\partial z}\,i\right]\right)_{j,k} \qquad (3.2c)$$

This method has a time step stability limit, but there is no rigorous stability analysis available for this. A conservative time step that is commonly used is

$$\Delta t < \min\left[\frac{|u|}{\Delta x} + \frac{|v|}{\Delta y} + \frac{|w|}{\Delta z} + c\quad\frac{1}{\Delta x^2} + \frac{1}{\Delta y^2} + \frac{1}{\Delta z^2}\right]^{-1} \qquad (3.3)$$

where c is the local speed of sound.

In the supersonic region, there exists a large gradient which requires a very fine mesh to resolve it. If they are not resolved, they produce a large oscillation which eventually blows up the solution. These oscillations of "low frequency" can be suppressed by adding a fourth order dampening. A common dampening used is the pressure dampening. This can be expressed in physical coordinates as

$$-\bar{\alpha}_\ell \Delta t_\ell \delta_\ell^3 \frac{\partial}{\partial\delta_\ell}\quad\frac{|v_\ell| + c}{4P}\quad\frac{\partial^2 p}{\partial^2\delta_\ell}\quad\frac{\partial U}{\partial\delta_\ell}\qquad \ell = 1,2,3 \qquad (3.4)$$

where $\delta_1 = \xi$, $\delta_2 = \eta$, and $\delta_3 = \zeta$.

4. INITIAL AND BOUNDARY CONDITIONS

In computational fluid dynamics the initial conditions usually correspond to a real initial situation for a transient problem, or a rough guess for a steady state problem. In practice, initial conditions are obtained from experiments, empirical relations, approximation theories, or previous computational results. An inappropriate initial guess may result in generating unphysically strong transient waves which propagate through the computational region dominating the flow field and eventually lead to a solution failure. In general, there are two important requirements that should be considered in the choice of initial conditions. First, they should be compatible with the fixed upstream boundary conditions. Secondly, the initial conditions should be as physically close as possible to the actual nature of the flow field in the region under study. The former will minimize the number of iterations required for convergence. An attractive approach is to initialize the entire flow field (including the upstream boundary and the body surface) with a crude and simple guess (e.g., free stream condition). Then, during the course of the computation, both body and upstream boundary conditions are changed in a gradual manner to their final values over a prescribed number of iterations. The former approach is applied in only one step which is equivalent to impulsive initial conditions.

It is equally important to implement a realistic, accurate, and stable method to determine boundary conditions. The application of certain conditions may cause numerical instability even though the flow is physically stable. There are neither mathematical nor physical justifications to implement a realistic boundary condition. Most of the boundary conditions currently implemented are drawn mainly upon intuition, wind tunnel experience, and computational experimentation. There are three general types of

boundary conditions. They are Dirichlet conditions (specified function value), Neumann conditions (specified normal gradient), and Robin conditions (a combination of both). Four important factors should be considered in the selection of boundary conditions. They are convergence, stability, computer time, and above all the physical justification.

For this problem there are five different boundary conditions. They are upstream, downstream, lateral, top, and solid boundary. The upstream boundary conditions are the undisturbed free stream conditions and are located at a grid space away from the leading edge, i.e.,

$$\bar{U}\Big|_{\text{upstream}} = \bar{U}_{\infty} \tag{4.1}$$

A zero gradient in y-direction (parallel to the primary direction of flow) is assumed for the downstream boundary, i.e.,

$$\frac{\partial \bar{U}}{\partial y}\Big|_{\text{downstream}} = 0 \tag{4.2}$$

The lateral boundaries are located far enough to avoid any influence on the interaction region. A boundary-layer profile can be prescribed on the lateral boundaries. These profiles can be obtained from their corresponding points of a flow over a flat pate. Presently, a zero gradient in z-direction is assumed for these boundaries, i.e.,

$$\frac{\partial \bar{U}}{\partial z}\Big|_{\text{lateral}} = 0 \tag{4.3}$$

The wall is assumed impermeable and no-slip boundary conditions are applied, therefore, all velocity components are assumed to be zero. The wall is also assumed to have a constant temperature Tw. A zero normal pressure gradient is assumed for the solid surface, i.e.,

$$\left.\frac{\partial P}{\partial n}\right|_{\text{solid}} = 0 \quad . \tag{4.4}$$

This evaluation may appear to be based on the boundary-layer approximation (zero normal pressure gradient). In fact, it is a much milder approximation, since constant pressure is not applied through the boundary layer but over one grid line in the boundary layer. This approximation has yielded stable computations for both non-separated and separated boundary layers [2]. From Eq. (A.25b), Eq. (4.4) can be expressed as

$$\frac{\partial P}{\partial n} = \frac{\xi_x n_x + \xi_y n_y + \xi_z n_z}{\left(n_x^2 + n_y^2 + n_z^2\right)^{1/2}} P_\zeta + \frac{n_x^2 + n_y^2 + n_z^2}{\left(n_x^2 + n_y^2 + n_z^2\right)^{1/2}} P_\eta + \frac{\zeta_x n_x + \zeta_y n_y + \zeta_z n_z}{\left(n_x^2 + n_y^2 + n_z^2\right)^{1/2}} P_\zeta = 0 \quad , \tag{4.5}$$

5. APPLICATION TO A BUTLER WING

As mentioned in the Introduction, the Butler Wing is a delta wing which was proposed by D. S. Butler [Ref. 4]. The planform of the body (Fig. 1a) is an isosceles triangle, and leading edges of the wing are laid along the Mach lines of the undisturbed stream. For the first 20% of the length, the body is a right circular core. The remainder of the body has elliptic sections which become more eccentric as the sharp trailing edges are approached (Fig. 1b). The semi major and minor axes are given by:

$$\text{Major axis (semi-span)} = \frac{x}{\beta} \qquad 0 \leq x \leq L \qquad (5.1a)$$

$$\text{Minor axis (thickness on centerline)} = \frac{x}{\beta} \qquad 0 \leq x \leq 0.2L \qquad (5.1b)$$

$$= \frac{x}{\beta}\left[1 - \left[\frac{x - 0.2L}{0.8L}\right]^4\right] \qquad 0.2 < x \leq L$$

where $\beta^2 = M_\infty^2 - 1$

The wing is symmetric about (XZ) and (XY) planes. This permits us to use only one quarter of the entire physical domain (Fig. 1C) which is extremely advantageous from computational viewpoint. However, if the angle of attack is greater than zero then half of the physical domain should be considered.

Some specific flowfield results have been obtained for the Butler wing and these are discussed in the next section.

6. RESULTS AND DISCUSSION

Grid generation is the very first-step which should be considered in obtaining flowfield solution over any configuration. Due to the data base management of our program, it is necessary to map the entire physical domain into a parallelepiped. Among the grid types, selection of an O-type grid would produce a point singularity at the tip and a line singularity along the trailing edge. Nevertheless, this maps the solid boundary onto an entire face of the parallelepiped. A C-type grid is used in the present work. However, the solid boundary is not mapped onto an entire face of the computational box. This creates a potential problem in updating the boundary conditions.

In this study, a two boundary grid generation (TBGG) technique developed by R. E. Smith [1] is used. The method is essentially an algebraic method. The application of the TBGG method requires that the entire body be sliced into different cross-sections (Fig. 2a-b). The cross-sections of wing are obtained in the stream-wise direction by analytical descriptions of the wing surface (Eq. 5.1). The TBGG method then is used to generate the grid for each station. There are fifty-five stations in the stream-wise direction, and each station has 64 x 36 grid points (Figs. 2c-2i). There is a total of 126,720 grid points which take 2.8 million 32-bit words of primary memory (16 variables). The computational time required is 1.9×10^{-5} sec/grid point/ iteration (2.5 sec/iteration). This is a typical requirement for the CYBER 205 with two pipes.

Results are obtained for a Butler wing at $M_\infty = 3.5$, $Re_\infty = 2 \times 10^6$/ft, $T_\infty = 390°R$, $Tw = 1092°R$, $L = 0.8$ ft, and zero angle of attack. The computed pressures are plotted in Fig. 3. The pressure coefficient along the center line is shown in Fig. 3a. The results are compared with available

experimental and numerical results (Refs. 4,6,7). The results are in excellent agreement with the experimental results of Ref. 4. Moreover, they are closer to the experimental results than previous numerical results (Refs. 4,6,7). Pressure ratios are plotted at constant chordwise position against the conical spanwise coordinates (41.66% and 68.33%). These are seen to be in good agreement with experimental and numerical results (Fig. 3b-c). There are, however, some discrepancies in the results between 30° and 60°. This might be due to the fact that grids are not orthogonal near those regions.

In the near future, extensive results will be obtained for different freestream conditions. These will be reported on in a future progress report.

7. CONCLUDING REMARKS

General formulations are presented to investigate the flowfield over complex configurations for high-speed freestream conditions. An advanced algebraic method is used to generate grids around these configurations. The computational procedure developed is applied to investigate the flowfield over a Butler wing. Illustrative results obtained for specified freestream conditions compare very well with available experimental and numerical results. Further studies, however, are needed to establish the validity and versatility of the present code. After such model validations, it is anticipated to use the code to investigate flowfield over complex configurations such as closed-bluff bodies (i.e., circular and elliptical cylinders on a flat plate, etc.).

REFERENCES

1. Smith, R.E., "Two-Boundary Grid Generation for the Solution of the Three-Dimensional Compressible Navier-Stokes Equations," NASA Technical Memorandum 83123, May 1981.

2. Roache, P.J., Computational Fluid Dynamics, Hermosa publisher, 1972.

3. MacCormack, R.W. and Bladwin, B.S., "A Numerical Method for Solving the Navier-Stokes Equations with Application to Shock-Boundary Layer Interactions," AIAA Paper 75-1, AIAA 13th Aerospace Sciences Meeting, Pasadena, CA, January 20-22, 1975.

4. Butler, D.S., "The Numerical Solution of Hyperbolic System of Partial Differential Equations in Three Independent Variables," Proceedings of the Royal Society, Series A Mathematical and Physical Sciences, No. 1281, vol 255, 232-252, April 1960.

5. Walkden, F. and Caine, P., "Surface Pressure on a Wing Moving with Supersonic Speed," Proceedings of Royal Society of London, Series A, volume 341, pp. 177-193, 1974.

6. Squire, L.C., "Measured Pressure Distributions and Shock Shapes on a Butler Wing," Cambridge University, Department of Engineering, CUED/A-Aero/TR9, 1979.

7. Squire, L.C., "Measured Pressure Distributions and Shock Shapes on a Simple Delta Wing," the Aeronautical Quarterly, volume 32, part 3, pp. 188-198, August 1981.

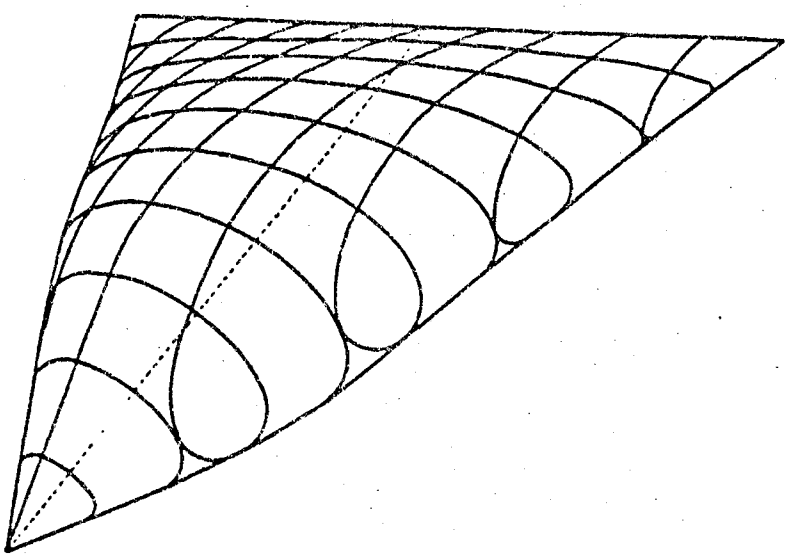

Figure 1a. Physical Model of a Butler Wing.

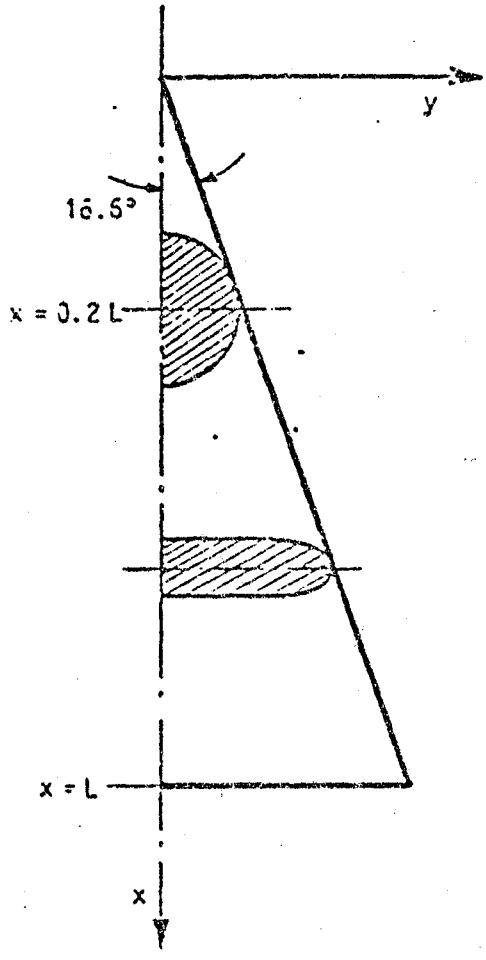

Figure 1b. Cross-section of the Butler Wing along streamwise direction.

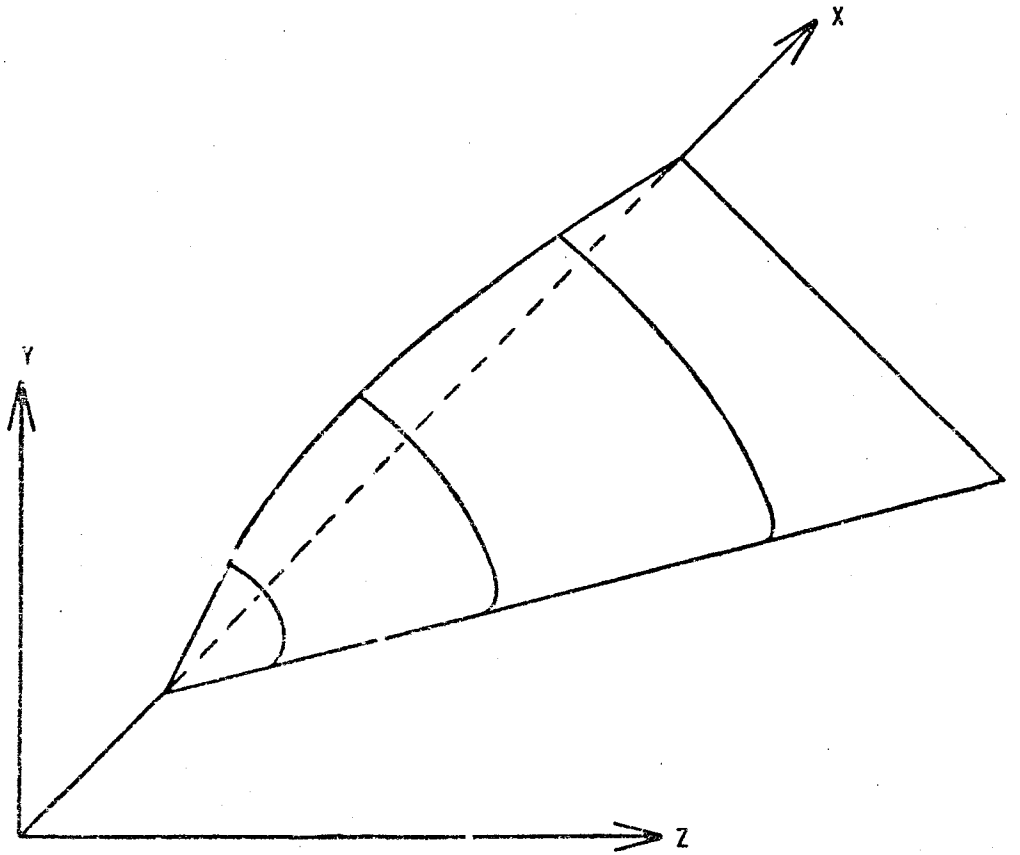

Figure 1c. Coordinate system for the Butler Wing.

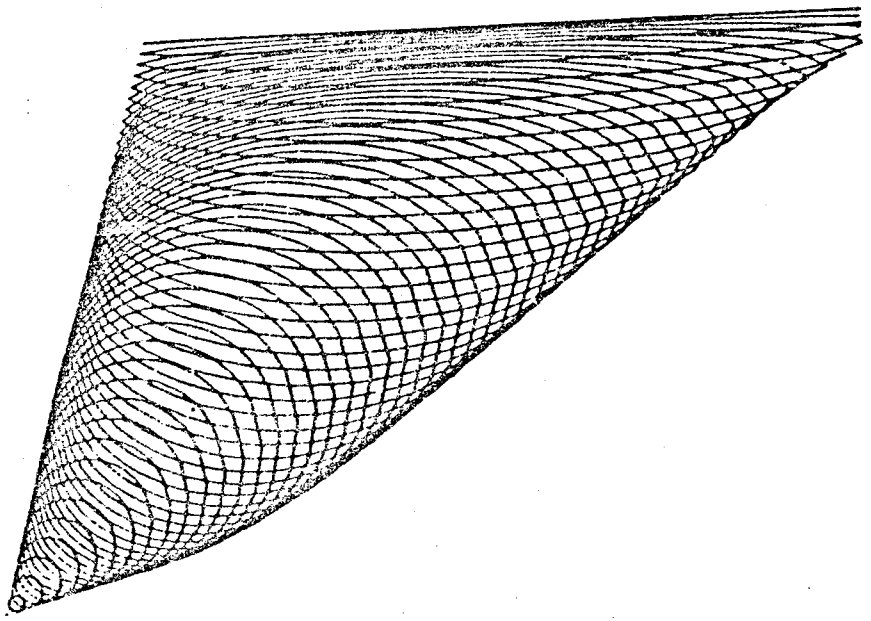

Figure 2a. Grid arrangement for the Butler Wing.

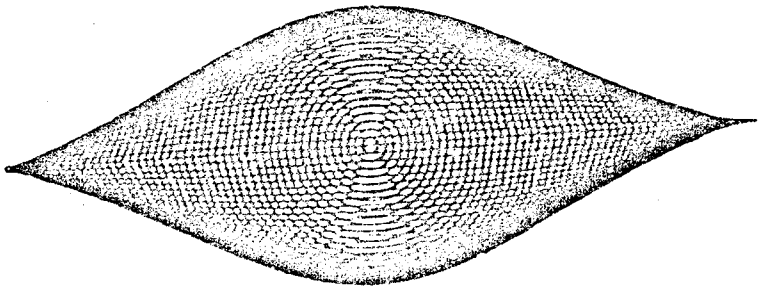

Figure 2b. Grid arrangement viewed from the origin.

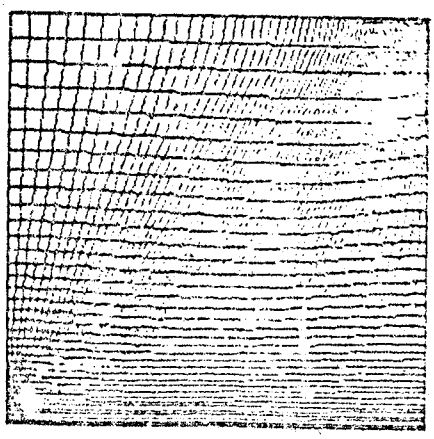

Figure 2c. Grid distribution of Station One.

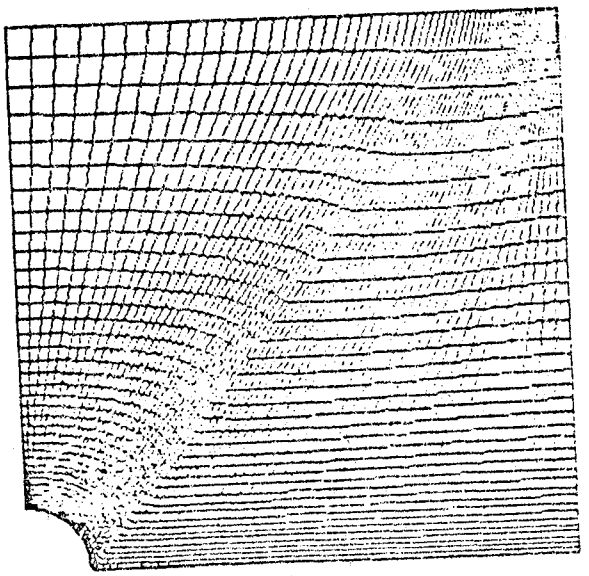

Figure 2d. Grid distribution at Station Eleven.

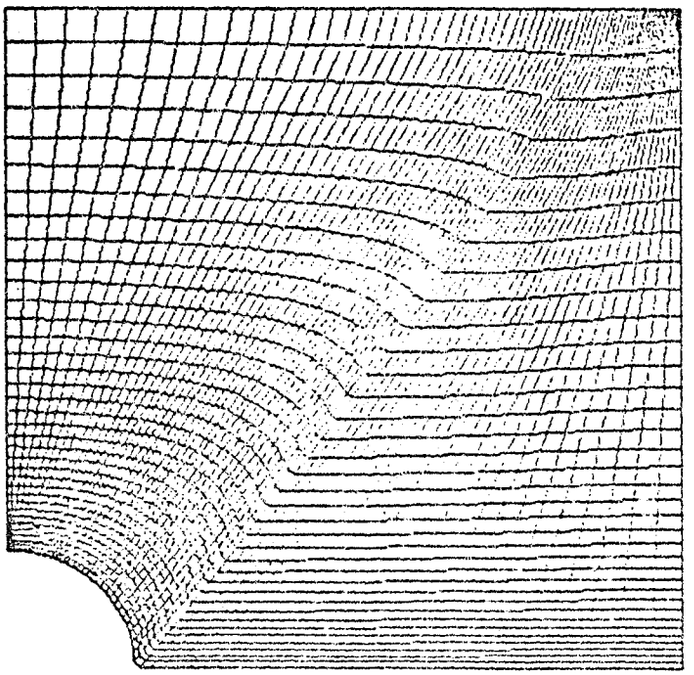

Figure 2e. Grid distribution at Station Sixteen.

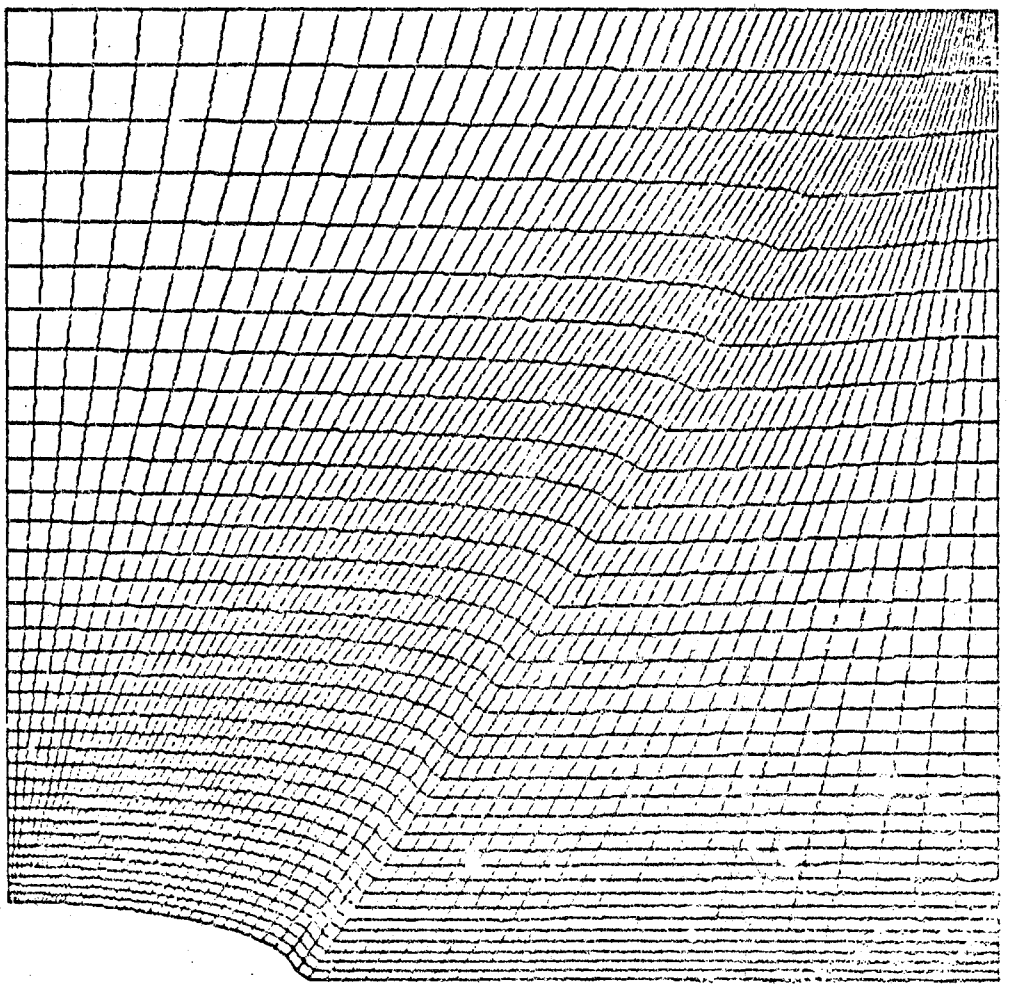

Figure 2f. Grid distribution at Station Twenty-six.

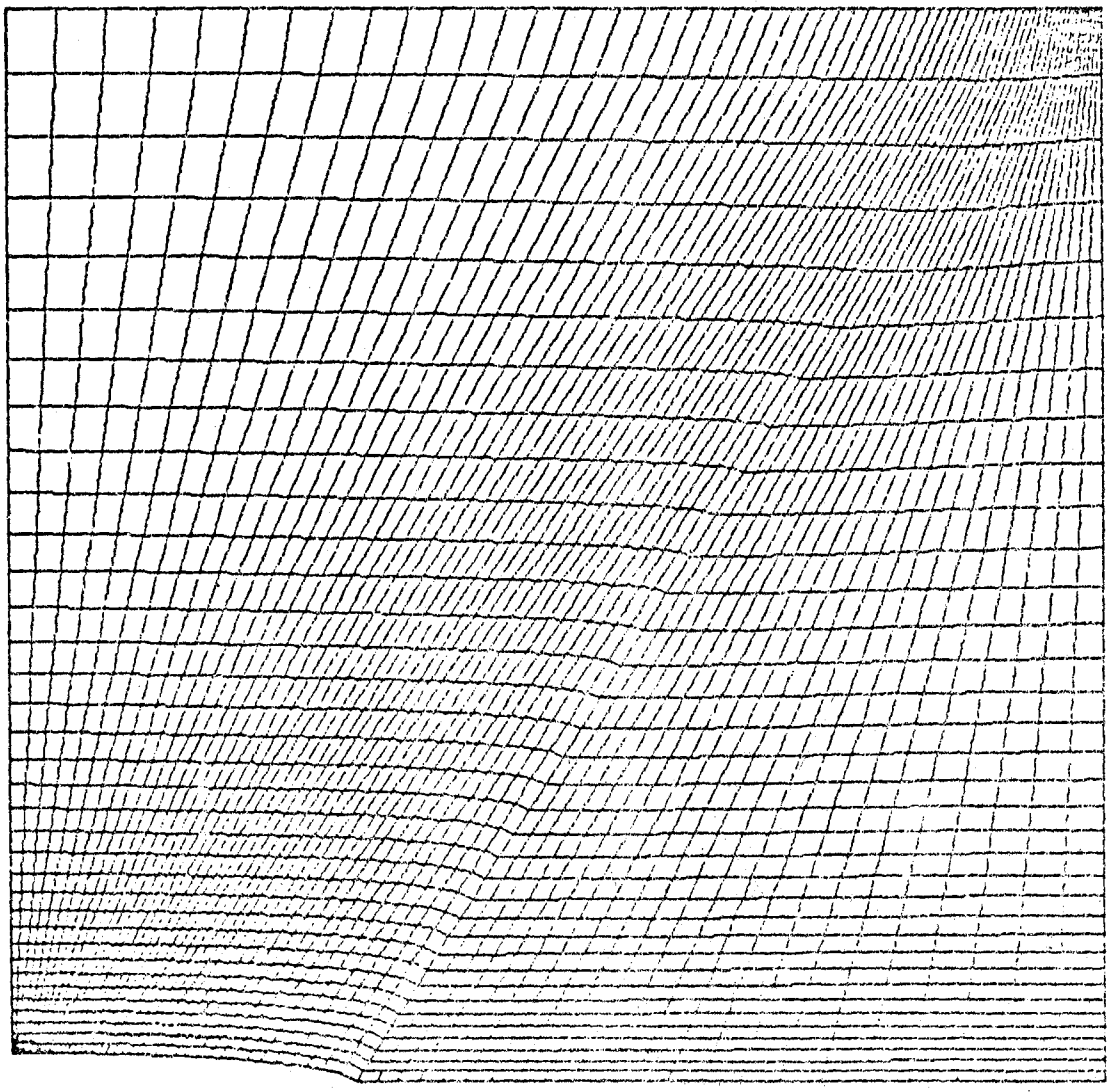

Figure 2g. Grid distribution at Station Thirty-one.

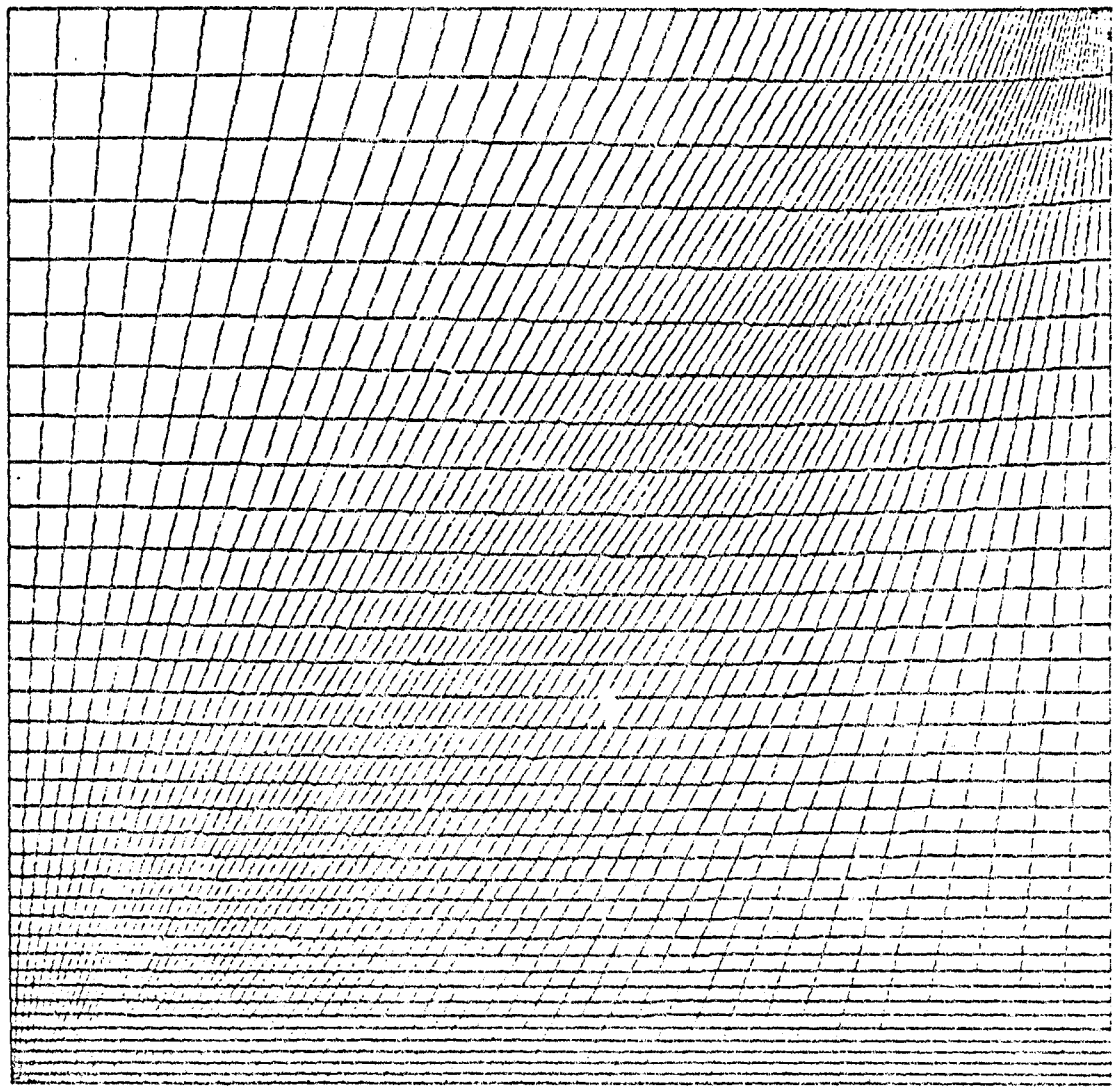

Figure 2h. Grid distribution at Station Thirty-six.

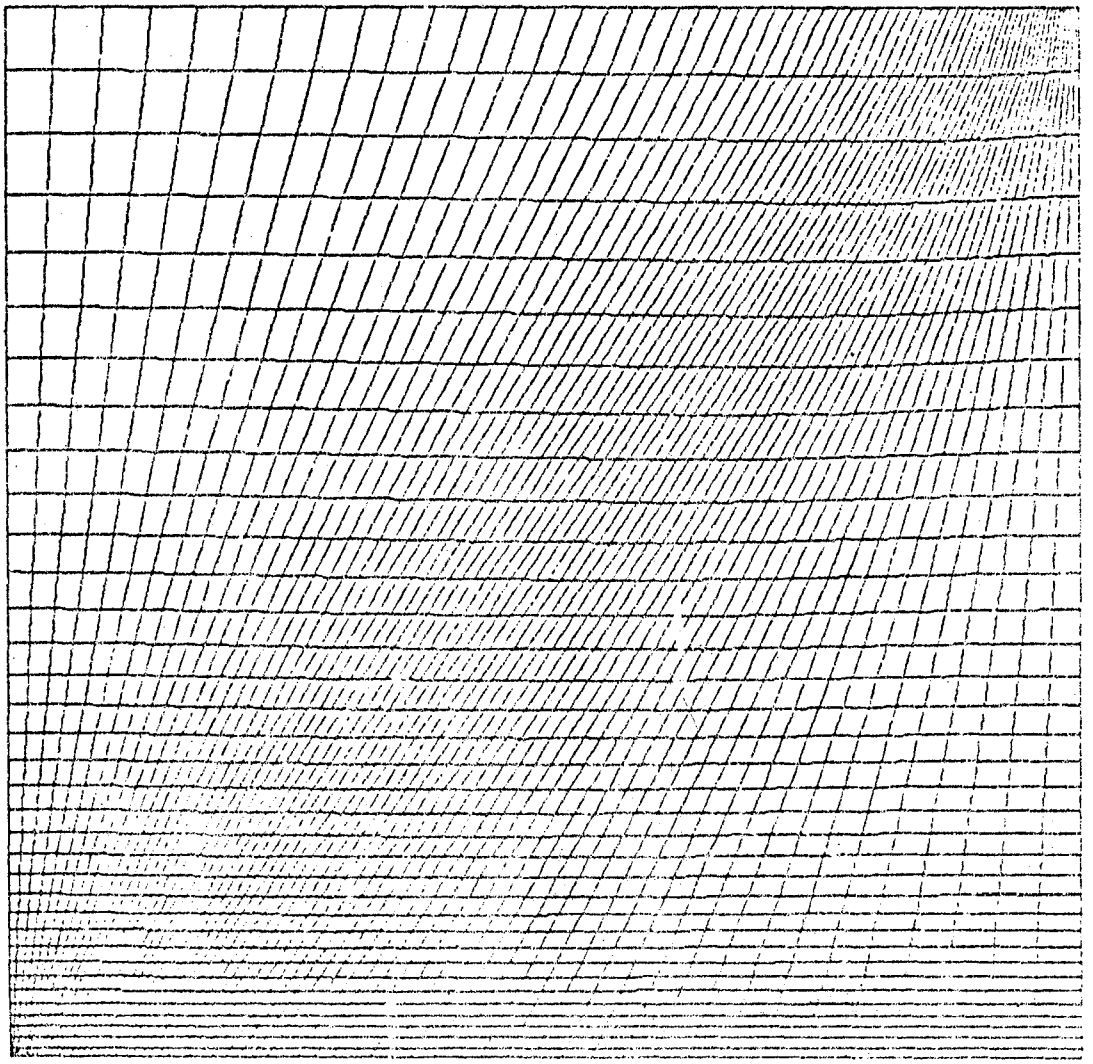

Figure 2i. Grid distribution at Station Forty-one.

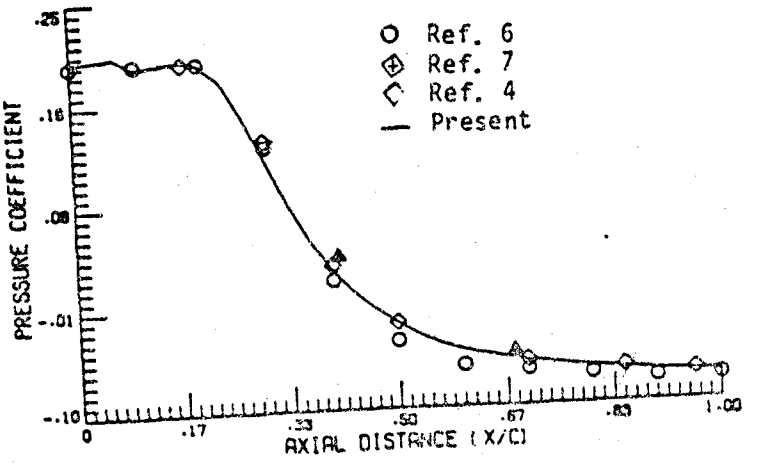

Figue 3a. Pressure coefficient along the center line.

Ref. 4 (computed)
Ref. 4 (experiment)
Present

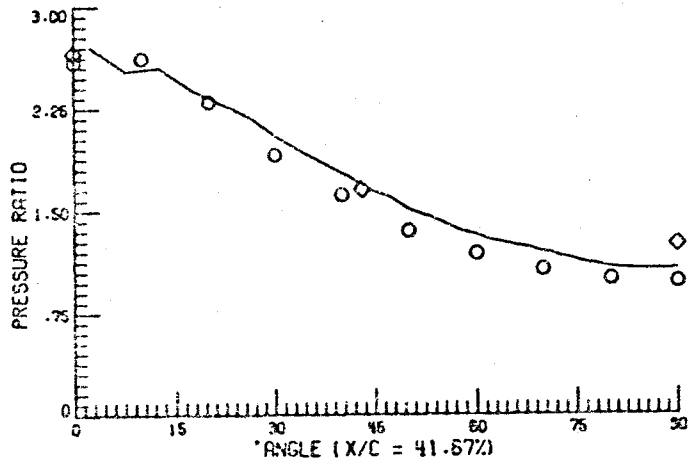

Fig. 3b. Pressure ratio at 41.67% of chord.

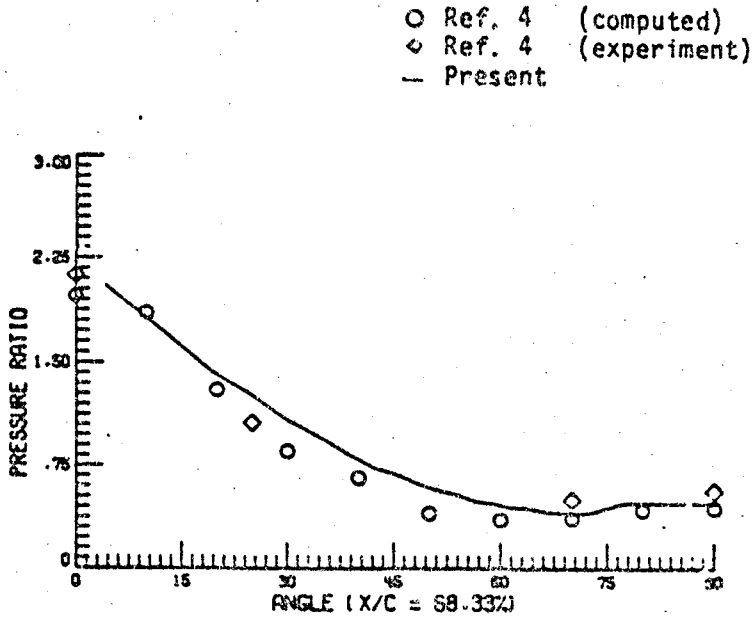

Figure 3c. Pressure ratio at 68.33% of chord.

APPENDIX A

MATHEMATICAL DETAILS FOR THE GOVERNING EQUATIONS

A.1 Curvilinear Coordinates

In covariant coordinates system (x_i), the position vector of a point from the origin is expressed as

$$\underline{r} = \underline{e}_i \, x_i = e_1 \, x_1 + e_2 \, x_2 + e_3 \, x_3 \qquad (A.1)$$

where e_i is the covariant base vector.

In the present study, covariant coordinates are labeled x, y, and z, and contravariant coordinates are labeled ξ, η and ζ. The covariant base vectors are defined as

$$\underline{e}_i = \frac{\partial r}{\partial x^i}$$

or

$$\begin{Bmatrix} e_1 \\ e_2 \\ e_3 \end{Bmatrix} = \begin{bmatrix} X_\xi & Y_\xi & Z_\xi \\ X_\eta & Y_\eta & Z_\eta \\ X_\zeta & Z_\zeta & Z_\zeta \end{bmatrix} \begin{Bmatrix} \bar{i} \\ \bar{j} \\ \bar{k} \end{Bmatrix} = [J^{-1}]^T \begin{Bmatrix} \bar{i} \\ \bar{j} \\ \bar{k} \end{Bmatrix} \qquad (A.2)$$

where J is the Jacobian of transformation. Magnitude of Jacobian $(|J|)$ is the local value of the ratio of an elemental volume in the physical (usually distorted) cell to the corresponding elemental volume in the mapped (cubic) cell.

The contravariant base vectors are defined as

$$\underline{e}^i = \frac{\partial r}{\partial x_i}$$

or

$$\begin{bmatrix} e_1 \\ e_2 \\ e_3 \end{bmatrix} = \begin{bmatrix} \xi_x & \xi_y & \xi_z \\ \eta_x & \eta_y & \eta_z \\ \zeta_x & \zeta_y & \zeta_x \end{bmatrix} \begin{Bmatrix} \bar{i} \\ \bar{j} \\ \bar{k} \end{Bmatrix} = [J] \begin{Bmatrix} \bar{i} \\ \bar{j} \\ \bar{k} \end{Bmatrix} \qquad (A.3)$$

Position vector can be expressed explicitly in terms of contravariant vector (x^i); however the infinitesimal vector $\underline{dr}$ can be expressed as

$$\underline{dr} = \frac{\partial r}{\partial x^i} \, d x^i = e_i \, dx^i \qquad (A.4)$$

also the magnitude of arclength (ds) can be expressed as

$$(ds)^2 = dr_o dr = \delta_{k\ell} dx^k dx^\ell \qquad (A.5)$$

where $\delta_{k\ell}$ is the kronecker delta,

$\delta_{kl} = 1$ if $k = \ell$

$\delta_{kl} = 0$ if $k \neq \ell$.

Substitution of Eq. A.4 into Eq. A.5 will result in

$$ds^2=(e_i \cdot e_j)dx_i dx_j=g_{ij}dx_i dx_j \tag{A.6}$$

where g_{ij} is called covariant fundamental metric coefficients.

These coefficients can be defined as

$$g_{ij} = [J^{-1}]^T [J^{-1}] = \frac{\partial x^k}{\partial x_i} \cdot \frac{\partial x^k}{\partial x_j} \tag{A.7}$$

They are defined as

$$g_{11} = x_\xi^2 + y_\xi^2 + z_\xi^2 \tag{A.8a}$$

$$g_{12} = g_{21} = x_\xi x_\eta + y_\xi y_\eta + z_\xi z_\eta \tag{A.8b}$$

$$g_{13} = g_{31} = x_\xi x_\zeta + y_\xi y_\zeta + z_\xi z_\zeta \tag{A.8c}$$

$$g_{22} = x_\eta^2 + y_\eta^2 + z_\eta^2 \tag{A.8d}$$

$$g_{23} = g_{32} = x_\eta x_\zeta + y_\eta y_\zeta + z_\eta z_\zeta \tag{A.8e}$$

$$g_{33} = x_\zeta^2 + y_\zeta^2 + z_\zeta^2 \tag{A.8f}$$

Similarly, covariant fundamental metric coefficients are defined as

$$g^{ij} = e_i \cdot e_j = [J][J]^T = \frac{\partial x_k}{\partial x^i} \cdot \frac{\partial x_k}{\partial x^j} \tag{A.9}$$

or

$$g^{11} = \xi_x^2 + \xi_y^2 + \xi_z^2 \tag{A.10a}$$

$$g^{21} = g^{12} = \xi_x \eta_x + \xi_y \eta_y + \xi_z \eta_z \tag{A.10b}$$

$$g^{13} = g^{31} = \xi_x \zeta_x + \xi_y \zeta_y + \xi_z \zeta_z \tag{A.10c}$$

$$g^{22} = \eta_x^2 + \eta_y^2 + \eta_z^2 \tag{A.10d}$$

$$g^{23} = g^{32} = \eta_x \zeta_x + \eta_y \zeta_y + \eta_z \zeta_z \tag{A.10e}$$

$$g^{33} = \zeta_x^2 + \zeta_y^2 + \zeta_z^2 \tag{A.10f}$$

Furthermore, there exists a unique relationship between contravariant and covariant fundamental metric coefficients,

$$g^{ij} = \frac{g_{rs}\, g_{ls} - g_{rt}\, g_{ls}}{|g_{ij}|} = \frac{G_{ij}}{|g_{ij}|} \tag{A.11}$$

where

$$G_{11} = g_{22}\, g_{33} - g_{23}^2 \tag{A.12a}$$

$$G_{12} = G_{21} = g_{13}\, g_{23} - g_{12}\, g_{33} \tag{A.12b}$$

$$G_{13} = G_{31} = g_{12}\, g_{23} - g_{13}\, g_{22} \tag{A.12c}$$

$$G_{22} = g_{11}\, g_{33} - g_{13}^2 \tag{A.12d}$$

$$G_{23} = G_{32} = g_{12}\, g_{13} - g_{23}\, g_{33} \tag{A.12e}$$

$$G_{33} = g_{11}\, g_{22} - g_{12}^2 \tag{A.12f}$$

There is also a relationship between covariant and contravariant base vector

$$\underline{e}^i = \frac{\underline{e}_j \times \underline{e}_k}{|g_{ij}|} \tag{A.13}$$

where $|g_{ij}| = |J^{-1}|^2$

i.e.

$$e^1 = \frac{(y_\eta z_\zeta - y_\zeta z_\eta)\, i - (x_\eta z_\zeta - x_\zeta z_\eta)\, j + (x_\eta y_\zeta - x_\zeta y_\eta) k}{|J^{-1}|}$$

or

$$\begin{bmatrix} e^1 \\ e^2 \\ e^3 \end{bmatrix} = \frac{1}{|J^{-1}|} \begin{bmatrix} (y_\eta z_\zeta - y_\zeta z_\eta) & -(x_\eta z_\zeta - x_\zeta z_\eta) & (x_\eta y_\zeta - x_\zeta y_\eta) \\ -(y_\xi z_\zeta - y_\zeta z_\xi) & (x_\xi z_\zeta - x_\zeta z_\xi) & -(x_\xi y_\zeta - x_\zeta y_\xi) \\ (x_\xi y_\eta - x_\eta y_\xi) & -(x_\xi z_\eta - x_\eta z_\xi) & (x_\xi y_\eta - x_\eta y_\xi) \end{bmatrix} \qquad (A.14)$$

where $J = \underline{e}^i$

There is also a relationship between contravariant and covariant base vectors

$$\underline{e}_i = \frac{\underline{e}^j \times \underline{e}^k}{|g^{ij}|}$$

where $|g^{ij}| = |J|^2$ (A.15)

i.e.

$$\begin{bmatrix} \underline{e}_1 \\ \underline{e}_2 \\ \underline{e}_3 \end{bmatrix} = \frac{1}{|J|} \begin{bmatrix} (\eta_y \zeta_z - \eta_z \zeta_y) & -(\eta_x \zeta_z - \eta_z \zeta_x) & (\eta_x \zeta_y - \eta_y \zeta_x) \\ -(\xi_y \zeta_z - \xi_z \zeta_y) & (\xi_x \zeta_z - \xi_z \zeta_x) & -(\xi_x \zeta_y - \xi_y \zeta_x) \\ (\xi_y \eta_z - \xi_z \eta_y) & -(\xi_x \eta_z - \xi_z \eta_x) & (\xi_z \eta_y - \xi_y \eta_x) \end{bmatrix} \qquad (A.16a)$$

or

$$[J^{-1}] = [e_1 \quad e_2 \quad e_3]^T$$

$$= \begin{bmatrix} (\eta_y\zeta_z - \eta_z\zeta_y) & -(\xi_y\zeta_z - \xi_z\zeta_y) & (\xi_y\eta_z - \xi_z\eta_y) \\ -(\eta_x\zeta_z - \eta_z\zeta_x) & (\xi_x\zeta_z - \xi_z\zeta_x) & -(\xi_x\eta_z - \xi_z\eta_x) \\ (\eta_x\zeta_y - \eta_y\zeta_x) & -(\xi_x\zeta_y - \xi_y\zeta_x) & (\xi_z\eta_y - \xi_y\eta_x) \end{bmatrix} \tag{A.16b}$$

The relationship between vector bases can be obtained also by matrix algebra. From basic matrix identity, it can be written as

$$[J] = [J^{-1}] = \frac{\text{Transpose of cofactor } [J^{-1}]}{|J^{-1}|} = \frac{[[J^{-1}]^*]^T}{|J^{-1}|} \tag{A.17}$$

Equation (A.17) is the same as Eq.(A.14).

There exists an inverse relation for Eq. (A.17).

A.2 Vector Representation in Curvilinear Coordinates

A vector $F(F_x\, i, F_y j, F_z\, k)$ can be expressed in a contravarient coordinates as

$$F_i = (g_{ii})^{1/2} F^i \tag{A.18}$$

where

$$F^i = \frac{\partial x^i}{\partial x} F_x + \frac{\partial x^i}{\partial y} F_y + \frac{\partial x^i}{\partial z} F_z \tag{A.19}$$

Equation (A.19) can be expanded as

$$\begin{bmatrix} \bar{F}_\xi / (g_{11})^{1/2} \\ \bar{F}_\eta / (g_{22})^{1/2} \\ \bar{F}_\zeta / (g_{33})^{1/2} \end{bmatrix} = \begin{bmatrix} \xi_x & \xi_y & \xi_z \\ \eta_x & \eta_y & \eta_z \\ \zeta_x & \zeta_y & \zeta_z \end{bmatrix} \begin{Bmatrix} F_x \\ F_y \\ F_z \end{Bmatrix} = [J] \begin{Bmatrix} F_x \\ F_y \\ F_z \end{Bmatrix} \qquad \text{(A.20)}$$

where g_{ij} is defined in Eq. (A.8).

The inverse relation to Eq. (A.20) is

$$\begin{Bmatrix} F_x \\ F_y \\ F_z \end{Bmatrix} = [J^{-1}] \begin{Bmatrix} \bar{F}_\xi / (g_{11}^{1/2}) \\ \bar{F}_\eta / (g_{22}^{1/2}) \\ \bar{F}_\zeta / (g_{33}^{1/2}) \end{Bmatrix} \qquad \text{(A.21)}$$

For example, velocity vector in covariant coordinates can be written as

$$\begin{Bmatrix} u \\ v \\ w \end{Bmatrix} = [J]^{-1} \begin{Bmatrix} U/(g_{11}^{1/2}) \\ V/(g_{22}^{1/2}) \\ W/(g_{33}^{1/2}) \end{Bmatrix}$$

Also, velocity vector in contravariant coordinates can be expressed as

$$\begin{Bmatrix} U/(g_{11})^{1/2} \\ V/(g_{22})^{1/2} \\ W/(g_{33})^{1/2} \end{Bmatrix} = [J] \begin{Bmatrix} u \\ v \\ w \end{Bmatrix}$$

Where u and U are velocities in covariant and contravariant coordinates system.

A.3 Normal Derivative in Curvilinear Coordinates

A normal derivative of a scalar variable can be computed as

$$\left(\frac{\partial A}{\partial n}\right)^{i} = n \cdot \nabla A \qquad \text{(A.23a)}$$

where

$$n = \frac{\nabla S}{|\nabla S|} = \frac{e_i}{|e_i|} \qquad \text{(A.23b)}$$

$$\nabla A = A_x\, i + A_y\, j + A_z\, K \qquad \text{(A.23c)}$$

or

$$\begin{Bmatrix} A_x\, i \\ A_y\, j \\ A_z\, k \end{Bmatrix} = [J]^T \begin{Bmatrix} A_\xi \\ A_\eta \\ A_\zeta \end{Bmatrix}. \qquad \text{(A.24a)}$$

Equation (A.23a) can be written as

$$\left.\frac{\partial A}{\partial n}\right|_{\text{constant } \psi} = \frac{[\psi_x\ \psi_y\ \psi_z]\ [J]^T}{(\psi_x^2 + \psi_y^2 + \psi_z^2)^{1/2}} \begin{Bmatrix} A_\xi \\ A_\eta \\ A_\zeta \end{Bmatrix} \qquad \text{(A.24b)}$$

For constant - ξ, Eq. (A.24b) can be written as

$$\left.\frac{\partial A}{\partial n}\right|_{\xi} = \frac{g^{11} A_{\xi} + g^{12} A_{\eta} + g^{13} A_{\zeta}}{\left(g^{11}\right)^{1/2}} . \qquad (A.25a)$$

For constant - n. Eq. (A.24b) can be written as

$$\left.\frac{\partial A}{\partial n}\right|_{n} = \frac{g^{21} A_{\xi} + g^{22} A_{\eta} + g^{23} A_{\zeta}}{\left(g^{22}\right)^{1/2}} . \qquad (A.25b)$$

For constant - ζ , Eq. (A.24b) can be written as

$$\left.\frac{\partial A}{\partial n}\right|_{\zeta} = \frac{g^{31} A_{\xi} + g^{32} A_{\eta} + g^{33} A_{\zeta}}{\left(g^{33}\right)^{1/2}} \qquad (A.25c)$$

also,

$$(A)_n^i = \frac{e^i}{|e^i|} \cdot \nabla A = \frac{1}{|e^i|} \sum_{j=1}^{3} (e^i \cdot e^j) A_i^j$$

$$= \frac{1}{\left(g_{ii}\right)^{1/2}} \sum_{j=1}^{3} g^{ij} \frac{\partial A}{\partial x^i} \qquad (A.26)$$

e.g.

$$(A)_n^{\xi} = \frac{1}{g^{11}} \left[g^{11} A_{\xi} + g^{12} A_{\eta} + g^{13} A_{\zeta}\right]. \qquad (A.27)$$

A.4 Miscellaneous Relations

Angle between two grid lines is given by

$$\text{Cos } \theta_{ij} = \frac{g_{ij}}{|g_i \; || \; g_{jj}|}^{1/2} \qquad \text{(A.28)}$$

therefore for orthogonal grid, the following should be true,

$$g_{ij} = 0 \quad \text{for} \quad i \neq j. \qquad \text{(A.29)}$$

Arclength is defined as

$$(ds)^2 = \sum_{i=1}^{3} \sum_{j=1}^{3} g_{ij} \; dx^i \, dx^j. \qquad \text{(A.30a)}$$

Arclength along x^i coordinate is defined as

$$(ds)^i = (g_{ii})^{1/2} \, dx^i. \qquad \text{(A.30b)}$$

The area of an element on which the x^i is constant is defined as

$$(dr^i = | \underline{e}_j \, d x^j \times \underline{e}_k \, d x^k | = (g_{ij}) \, dx^i \, dx^j \qquad \text{(A.31)}$$

e.g.

$$dr^{\xi} = | e_2 \, d\eta \times e_3 \, d \zeta | = G_{11} \, d\eta \, d\zeta \qquad \text{(A.32a)}$$

$$dr^{\eta} = G_{22} \, d\xi \, d\zeta \qquad \text{(A.32b)}$$

$$dr^{\zeta} = G_{33}\, d\xi\, d\eta. \qquad (A.32c)$$

Volume of an element is defined as

$$dV = \frac{\partial(x,y,z)}{d(\xi,\eta,\zeta)} = |J^{-1}|\, d\xi\, d\eta\, d\zeta$$

$$= |e_1\ (e_2 \times e_3)|\, d\xi\, d\eta\, d\zeta = (|g_{ij}|)^{1/2}\, d\xi\, d\eta\, d\zeta \qquad (A.33)$$

END

DATE

FILMED

JAN 22 1986